Worcester Polytechnic Institute

Examining the Effects of Chromium III and VI on Stress Granules

A Major Qualifying Project
Submitted to the Faculty of
Worcester Polytechnic Institute
in partial fulfillment of the requirements for the
Degree in Bachelor of Science
in
Biology and Biotechnology
by

Bulent Furkan Atahan

Vivian Nguyen

Date: May 2021
Project Advisor:

Dr. Natalie Farny, Advisor

Abstract

The health effects of chromium exposure remain unclear, although humans are exposed to chromium, a toxic metal, through food and water consumption and inhalation of contaminated air. In general, chromium VI exposure has increased risks than chromium III exposure as it is more commonly associated with human disease and cancer. While many studies have examined the effects of Cr III and VI on cellular toxicity, little is known about the cellular stress mechanisms activated by these two variants of chromium. Therefore, in this project, we investigated the specific pathway of stress-induced translational control influenced by chromium. Since Cr VI has a higher toxicity than Cr III, we hypothesized that there would be a higher rate of cellular stress in response to Cr VI than Cr III. After analyzing the results from various acute exposure assays and Western blots, Cr VI generally formed more stress granules than Cr III. Chromium VI but not chromium III resulted in the phosphorylation of eIF2α, indicating an effect on translational arrest. Despite this, there wasn't a significant difference between stress granule formation caused by the two valence states of chromium to fully support the hypothesis. As result, this research will aid in understanding the effects of chromium III and VI on human cells.

Acknowledgements

We would like to thank our advisor, Professor Natalie Farny, for guiding and supporting us throughout this project. This paper and the research behind it would not have been possible without her valuable feedback and guidance.

Table of Contents

Background

Cellular Stress Response

Cells are exposed to and affected by stressors, originating from the environment, that cause a shift in their genetic and/or metabolic status. Normal conditions include environments containing sufficient amounts of nutrients, hormones and growth factors for cells to grow and expand and other environmental factors such as favorable temperature and acidity (Arora, 2020).

Some examples of potential stress factors are heat shock, toxicity, viral infections, and oxidative stress. These stressors damage the structure and function of the cell's macromolecules. The extent of damage depends on the particular cell and the type and intensity of the stress (Poljšak & Milisav, 2012; Abdulla & Campbell, 1997). Since macromolecules can be damaged, it is critical for cells to preserve their regulatory processes in the genomic, transcriptional, post-transcriptional, translational, and post-translational levels in order to maintain genomic integrity (Feng & Koh, 2003).

Cells react to stressors by activating the cellular stress response, which could widely range from induction of cell repair mechanisms to activation of pathways that promote survival to evoking programmed cell death to eliminate damaged cells (Fulda et al., 2010). In some cases, cells react to stressors by forming stress granules (SGs), but take many precautions to protect their viability. Initially the cell's response is focused on defending against and recovering from the stressor. If that defense is unsuccessful, a variety of cell death programs can be activated to eliminate damaged cells from the organism.

Stress Granules (SGs)

Stress granules were first discovered in mammalian cells in 1986 and is a relatively newer concept in biology and biochemistry (Collier & Schlesinger, 1986). SGs are non-membranous cytoplasmic aggregates in distinct structures that form in response to stress conditions. They are good models to better understand topics such as neurodegeneration, translational control, stress adaptation, and cell fate (Nostramo and Herman 2017). They contain non-translating messenger ribonucleoproteins (mRNPs), which are mRNAs with bound proteins (Anderson & Kedersha, 2002). In response to translation inhibition, mRNA that are bound by RNA-binding proteins accumulate and assemble into large cytoplasmic bodies (van Leeuwen and Rabouille, 2019). Within these granules lay bundles of translation initiation factors including eIF2α, eIF3, eIF4A/B, eIF4E, and eIF4G. Kinases activated by stress triggers the formation of SGs by phosphorylation of eIF2α (van Leeuwen and Rabouille, 2019). eIF2α kinase activation pathway is portrayed in Figure 1.

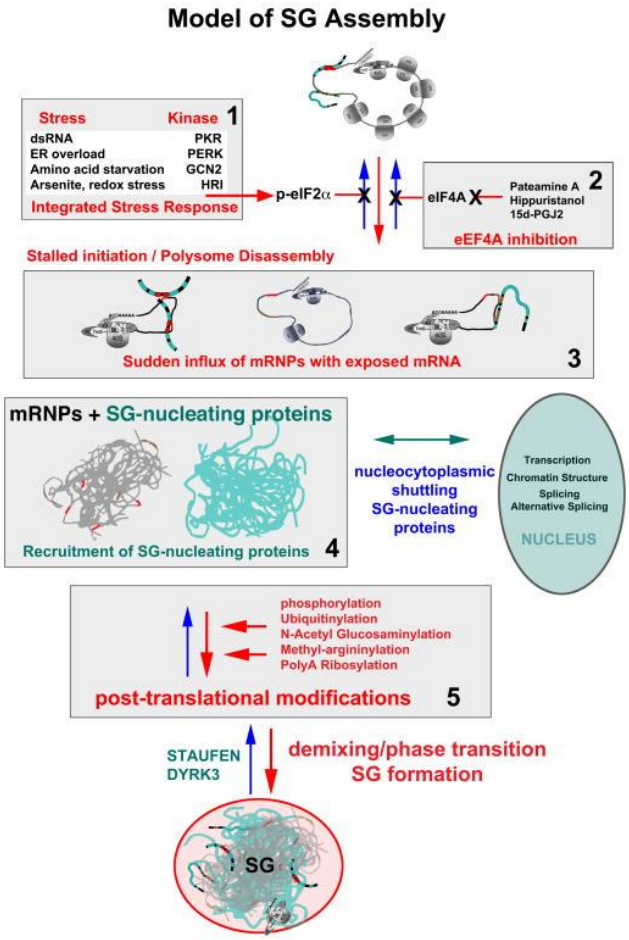

Figure 1: Stress granule and eIF2α kinase activation pathway (Anderson, Ivanov, and Kedersha 2013)

Rapid increase in non-polysomal mRNPs caused by stress related phosphorylation of eIF2α stagnates initiation rates. mRNPs lacking ribosomes have increased exposed mRNA areas and these mRNAs quickly bind to available mRNA binding proteins. mRNA/protein mixture is very active due to the fact that mRNA binding proteins always look for optimum binding sequences. Once this protein-mRNA mixture is ready, SGs are formed via post-translational modification and SGs are available to connect with proteins in various signalling pathways and mRNA functions. Some steps of SG formation happen simultaneously and not necessarily sequentially like in Figure 1.

Stress Response in Toxic Metals

Toxic metals present a substantial threat to cell survival as it normally requires a balance between molecular oxygen and various antioxidants, but toxic metals create an imbalance (Fulda, Gorman, Hori, & Samali, 2010). Oxidative stress is when the imbalance occurs and when it is

sustained, it can lead to cell death. Typically in cells, there is an equilibrium between abundant pro-oxidant species and antioxidant defense mechanisms, such as ROS-metabolizing enzymes and antioxidant proteins. These molecules work to keep the balance between molecular oxygen and antioxidants.

Humans are commonly exposed to toxic metals such as lead, cadmium, chromium, mercury, and arsenic since they are widely available in the environment through contaminated air, water, soil and food (Ercal et al. 2001). Redox-active metals include iron, copper, and chromium, and go through redox cycling, or repetitively coupled reduction and oxidation reactions that involve oxygen and reactive oxygen species (ROS) (Arner, 2012). On the other hand, redox-inactive metals, lead, cadmium, and mercury, deplete cells' antioxidants that are readily available to defend cells against stressors. Both types of metals are able to cause an increase in the production of ROS, which causes oxidative stress. Consequently, cells can form lesions caused by ROS, resulting in lipid, protein, and DNA damage. The oxidative stress caused by toxic metals is suggested to be partially responsible for the toxic effects of said metals.

Chromium III and VI

The element chromium occurs in the natural environment in rocks, animals, plants, soil, and volcanic dust and gases (epa.gov, 2000). There are two predominant valence states of chromium: it naturally exists as trivalent chromium (Cr III) and is commonly produced by industrial processes as hexavalent chromium (Cr VI). Cr III is an essential nutrient in the human diet as it promotes normal glucose, protein, and fat metabolism, but in excess has a toxic effect. In contrast, Cr VI is much more toxic than Cr III as it is known to cause lung cancer (epa.gov, 2000).

Humans are commonly exposed to chromium through consumption of food, drinking water, and inhaling contaminated air. Chromium is mainly used for making steel and other alloys, playing a part in chrome plating, the manufacture of dyes and pigments, leather and wood preservation, and treatment of cooling tower water (OSHA.gov). As chromium is added to alloy steel to increase hardenability and prevent corrosion, it causes high exposure to workers when welding stainless steel. Chromium disposal sites or manufacturing and processing plants can affect residents in the area as there is a higher chromium exposure than the general population. A study was conducted using trivalent/hexavalent concentration ratios and historic air-sampling data to determine the effects of cumulative chromium exposure on chromate production plant employees (Gibb, 2000). The researchers found that only cumulative hexavalent chromium exposure, and not trivalent, was associated with an increased lung cancer risk.

Once exposed, chromium targets the respiratory tract and in acute cases, it causes shortness of breath, coughing, and wheezing, whereas chronic exposure causes perforations and ulcerations of the septum, bronchitis, decreased pulmonary function, pneumonia, and additional respiratory debilitations (epa.gov, 2000). Human studies have established Cr VI is a human carcinogen and can cause lung cancer (Gibb, 2000). Similarly, animal studies have shown Cr VI inhalation exposure can cause lung tumors (Stearns, 1995). In efforts to detoxify and lower the level of Cr VI present in the human body, many bodily systems reduce Cr VI to Cr III. This results in decreased levels of Cr VI and increased levels of Cr III.

Relationship Between Chromium III and VI and Stress

Research on the oxidative stress response to Cr VI exposure for yeast revealed further insight on the toxic metal (Lazarova et al., 2014). In general, it decreased the mass of cells, indicating that the cells had enough stress to affect its growth and proliferation mechanisms. Acute and chronic exposure caused an increase in ROS generation, providing evidence that Cr VI was causing oxidative stress based on the imbalance between ROS and antioxidants. There was a greater increase for chronic exposure than acute. Another experiment looked into how metal exposure caused oxidative damage of proteins as it is a consequence of excessive ROS production. Acute exposure caused an increase in protein oxidation, but chronic exposure showed a lower increase comparatively. The researchers observed the effect of stress on the reserve carbohydrates as oxidative stress can cause damage to these molecules as well. Interestingly enough, the stress seemed to enhance and increase the glycogen levels, but on the other hand, there was damage and a decrease in trehalose levels. Lastly, they observed if the presence of metal ions stimulated enzyme antioxidants to defend itself, as the cells would attempt to restore the balance between ROS and antioxidants. They found that enzymes, specifically superoxide dismutase (SOD) and catalase (CAT), were activated in response to the elevated ROS levels when exposed to Cr VI (Lazarova et al., 2014).

There has also been research on Cr VI-induced oxidative stress resulting in apoptotic cell death and the effects of modulation on the p53 apoptotic regulatory gene (Bagchi et al. 2001). Cr VI has demonstrated its severity as DNA damage was induced following acute and chronic oral administration. Additionally, it induced a greater cytotoxicity comparatively to Cr III based on increased production of ROS, enhanced excretion of urinary lipid metabolites, and increased hepatic DNA-single strand breaks. It is hypothesized that this is due to the ability of Cr VI to penetrate biological membranes through non-specific anion carriers more readily than Cr III. To summarize, Cr VI demonstrated enhanced formation of ROS, decreased cell viability, increased cellular and genomic hepatic DNA fragmentation, enhanced intracellular oxidized states, membrane damage with leakage of lactate dehydrogenase, activation of protein kinase C, and apoptotic and necrotic cell death.

Examining the Effects of Chromium III and VI on Stress Granules

The cellular level effects of chromium III and VI, particularly related to the activation of cellular stress response pathways, are not well understood. Despite this, it is known that these toxic metals cause oxidative stress, where Cr VI is more toxic to cells than Cr III. Since oxidative stress leads to stress granule formation, we hypothesized that chromium would activate cellular stress response pathways and cause stress granules. Therefore, we predicted that Cr VI may cause more stress than Cr III. To test our hypothesis, we used fluorescence microscopy and western blotting to analyze stress granule formation and stress pathway activation in cells. Surprisingly, we find that neither Cr III nor Cr VI is associated with a significant increase in stress granules, although a very low level of stress granules are observed with Cr VI. However, we do find increased phosphorylation of eIF2α associated with Cr VI exposure which is not observed in response to Cr III. The results suggest Cr VI may be associated with activation of the cellular stress response, but warrant further investigation.

Materials and Methods

Cell Line Maintenance

Double-stable osteosarcoma (U2OS-DS) (DSMZ Cat# ACC-785, RRID:CVCL_0042) and HAP1 (RRID:CVCL_Y019) cells were maintained using complete DMEM media (88% DMEM, 10% FBS, 1% penicillin/streptomycin, 1% glutamine). Cells were incubated at 37°C with 5% CO_2 and sub-cultured 3 times a week, 2 to 3 days apart (Monday, Wednesday, Friday), at a ratio of 1:5 to 1:8 (U2OS-DS) or 1:10 to 1:15 (HAP1).

Acute Exposure Assays

U2OS-DS or HAP1 cells were plated around $1x10^5$ cells/well in a 12-well plate with coverslips where each well contained 1 mL of media. The plate was incubated for about 24 hours or less at 37°C and the variations of well plate organization are shown in Figure 2.

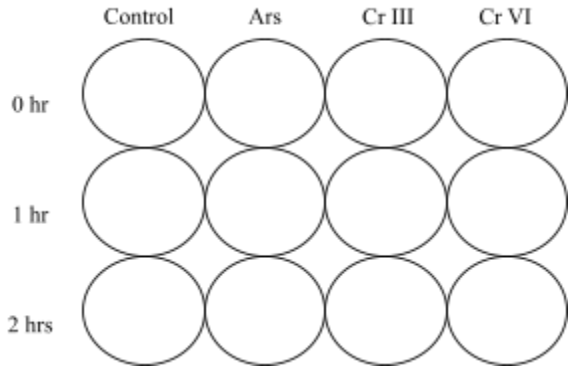

Figure 2: Well-plate organization of the acute exposure assay used for U2OS-DS and HAP1 cells.

Half of the pre-conditioned media in the wells (0.5 mL from each well; 6 mL total) were collected and divided into tubes depending on the treatment being applied. The media was then untreated, or treated with 50-500 μM of arsenite, 500 μM of Cr III, or 500 μM of Cr VI. The remaining media in the wells were aspirated and replaced with 0.5 mL of the respective treatment. After the well plate was incubated for 1 hour at 37°C, the media was disposed of and the wells were washed with non-sterile 1X PBS. After disposing of the PBS, 0.5 mL of paraformaldehyde was added to the wells and the plate was incubated at room temperature on the orbital shaker for 10 minutes. The paraformaldehyde was disposed and 0.5 mL of 100% methanol was added to the wells. The plate was on the orbital shaker for another 10 minutes at room temperature followed by a 1X PBS rinse. U2OS-DS were then mounted to microscopy slides using vinyl mounting media whereas HAP1 cells were stained (procedure below) then mounted. The coverslips were then mounted onto glass slides (two coverslips per slide) with

vinyl mounting media. The labels on the slides were blinded to reduce bias and the cells were viewed at 400X magnification. A minimum of 200 cells and 3 different fields were counted on each coverslip in order to calculate the percentage of cells positive for stress granules.

Staining Cells for Fluorescence Microscopy

Following the acute exposure assay and fixing the cells with paraformaldehyde, PBS was aspirated from each well, followed by adding 0.5 mL of 5% BSA and the plate was incubated at room temperature on the orbital shaker for 1 hour. The BSA was aspirated from each well and was replaced with 0.5 mL of the primary antibody solution (Table 1). The plate was incubated at room temperature on the orbital shaker for 1 hour followed by aspiration. The plate was washed 3 times with 1X PBS and it was placed on the orbital shaker for 5 minutes each time. PBS was aspirated and replaced each well with 0.5 mL of the secondary antibody solution (Table 1). The plate was incubated at room temperature on the orbital shaker for 1 hour followed by aspiration. The plate was washed 3 times with 1X PBS and it was placed on the orbital shaker for 5 minutes each time. The coverslips were then mounted as described above.

Western Blot from Acute Exposure Assay

An acute exposure assay without coverslips was performed on U2OS-DS cells with a plate arrangement as shown in Figure 2.

Sample Collection and Preparation:

The media was aspirated after being treated and the wells were rinsed twice with 1X PBS. After aspirating the remaining PBS, each well was treated with 100 µL of 1X SDS sample buffer and the plate was shaken by hand. The samples were collected from each well into labeled microcentrifuge tubes using a pipetman. The samples were then stored at -20˚C.

To prepare the samples, a needle (27-30 gauge) and syringe were used to pass the sample 10-15 times. New microcentrifuge tubes containing 20 µL of sample and 2 µL of DTT (100 mg/mL) were placed into a heating block at 75℉ for 10 minutes.

Gel Electrophoresis:

The samples were removed from the heating block and were centrifuged for 30 seconds. 15 µL of each sample was loaded into a polyacrylamide gel (4-20%, BioRad) and it was run at 120V for 90 minutes. To prepare the gel for blotting, it was removed and washed with distilled water. After being placed on the orbital shaker for 5 minutes, the distilled water was replaced with transfer buffer (0.5X Tris-Gly-MeOH).

Blotting:

The proteins from the gel electrophoresis were transferred to PVDF membrane by performing electroblotting at 100V for 90 minutes. The membrane was rinsed with wash buffer (0.05% Tween-20 in 1X PBS) followed by a blocking solution (5% dry milk and wash buffer). This was placed on the orbital shaker at room temperature for 1 hour. The blocking solution was disposed and the membrane was washed with wash buffer 3 times, each with 5 minutes on the orbital shaker. The membrane was then treated with primary antibody (Table 1) and was stored at 4˚C overnight. The membrane was washed with wash buffer 3 times as before and was treated with the secondary antibody solution (Table 1) to be left on the orbital shaker for 1 hour. The membrane was washed 5 times with wash buffer and was left on the orbital shaker for 5 minutes each time. After disposing the wash buffer, 1 mL of each developing solution (from SuperSignal West Pico Trial Kit, Product #34577) was added to the membrane. The blot was then imaged and analyzed using the BioRad Image Lab software.

Table 1: Antibodies and Dilutions Used in this Study

Antibody	**Application**	**Dilution**	**Manufacturer**	**Product #**
Rabbit-anti-G3BP1	Immunofluorescence primary stain	1 µL/1 mL of 5% BSA/PBS	Abcam	AB181150
Anti-rabbit IgG Alexa 594 (red)	Immunofluorescence secondary stain	0.5 µL/1 mL of 5% BSA/PBS	Cell Signaling Technologies	8889S
Hoechst 33342 (blue) nuclear stain	Immunofluorescence secondary stain	0.2 µL/1 mL of 5% BSA/PBS	Thermo Scientific	62249
Rabbit-anti-p-eIF2α	Western Blot primary stain	1:1,000	Cell Signaling Technologies	3398S
eIF2α-antibody D7D3	Western Blot primary stain	1:500	Cell Signaling Technologies	5324T
Anti-rabbit IgG HRP-linked	Western Blot secondary stain	1:10,000	Cell Signaling Technologies	7074P2

Results

Chromium III, Chromium VI, and Arsenite Acute Exposure Comparison Assay

An acute exposure assay was performed on U2OS-DS cells to calculate the average percent positive of stress granule formation under the treatment of 500 µM Cr III, Cr VI, or arsenite. Arsenite was assigned as the positive control treatment since it is known to produce a high cellular stress response and thus a high average percent positive. No treatment was applied to the control wells. As shown in Figure 3, when viewed under the fluorescent microscope, cells responded more actively to Cr VI treatment, in which 4.7% of the cells formed stress granules and 1.6% of cells treated with Cr III formed stress granules. This result was consistent with our background research which showed that Cr VI was more toxic to mammalian cells than Cr III. All three experiments performed had consistent results as shown by the miniscule error bars and proximity of the data points. The control cells had little to no stress granule formation. The positive control, arsenite, almost always had 100% positive results.

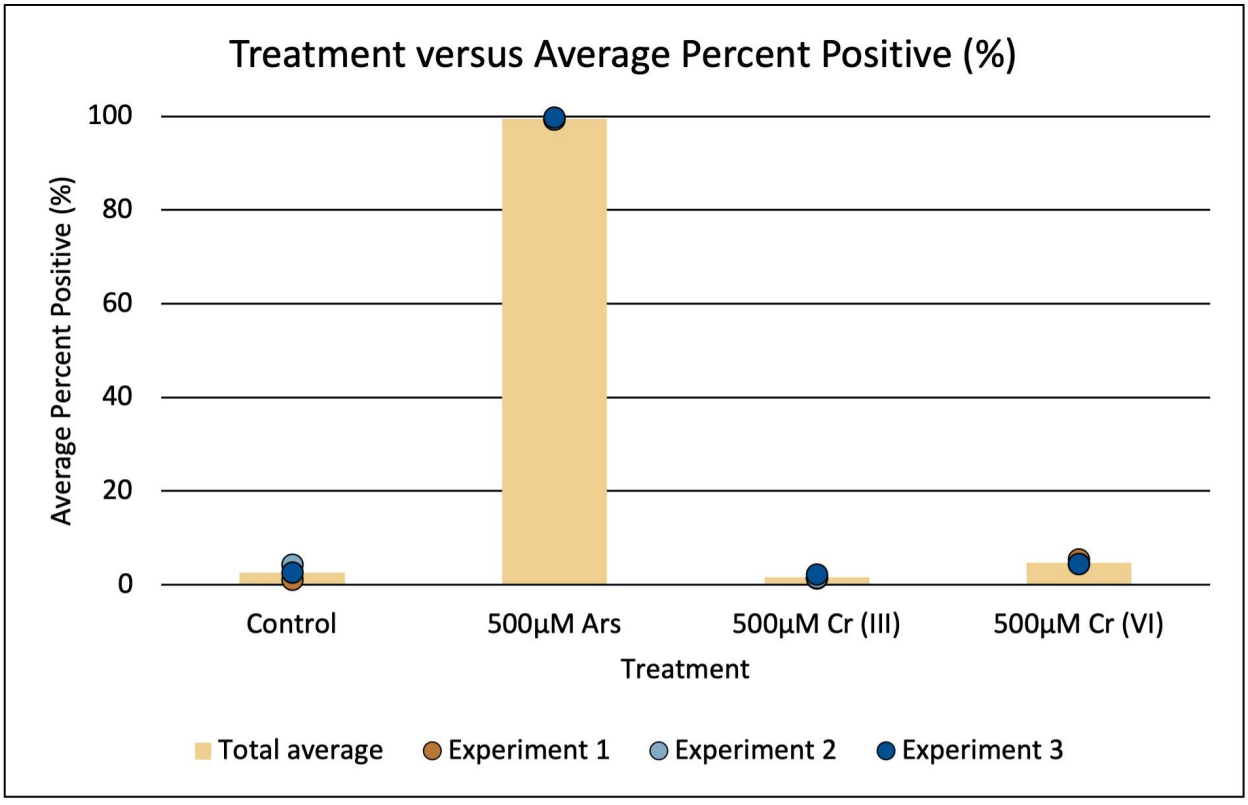

Figure 3: Stress granule formation in response to acute exposure of U2OS-DS cells to chromium III and VI. Cells were treated with 500 µM solutions of the indicated treatments for 1 hour and 3 replicates were performed. Error bars represent standard error and data points for each experiment are marked on the bars.

Hourly Acute Exposure Comparison Assay

Based on the results from Figure 3, it was hypothesized that cells would form more stress granules as time passes. If the cells were given more time to be exposed to the stress condition, they may form a greater amount of stress granules. In order to observe a gradual increase in stress granule formation, the treatments were applied to the cells at 0, 1, or 2 hours in a similar fashion as the prior experiment. In this experiment 50 μM of arsenite was used instead of 500 μM to closely observe the threshold change in stress granule formation. Again, arsenite was a positive control and the negative control had no treatment applied. In Figure 4, it can be seen that most of the treatments form more stress granules with greater amounts of time. The negative control showed little to no stress granule formation until the 2 hour time point. This was due to an unexpected greater average percent positive for Experiment 5, which is indicated by the dark blue data point and the according error bar. The positive control provided supporting evidence for our hypothesis where the stress granule formation increased with time. Since 50 μM is near the threshold for stress granule formation, there was a wide range of results, which is indicated by the data points and according error bars. The Cr III treatment does not support the hypothesis since stress granule formation was incredibly low and no trend could be determined. The average percentages positive for all three time points were under 2%, therefore it is not conclusive whether this treatment decreases over time or remains consistent. The Cr VI treatment supports the hypothesis and shows a clear increase in stress granule formation over time, changing from roughly 1 to 5%.

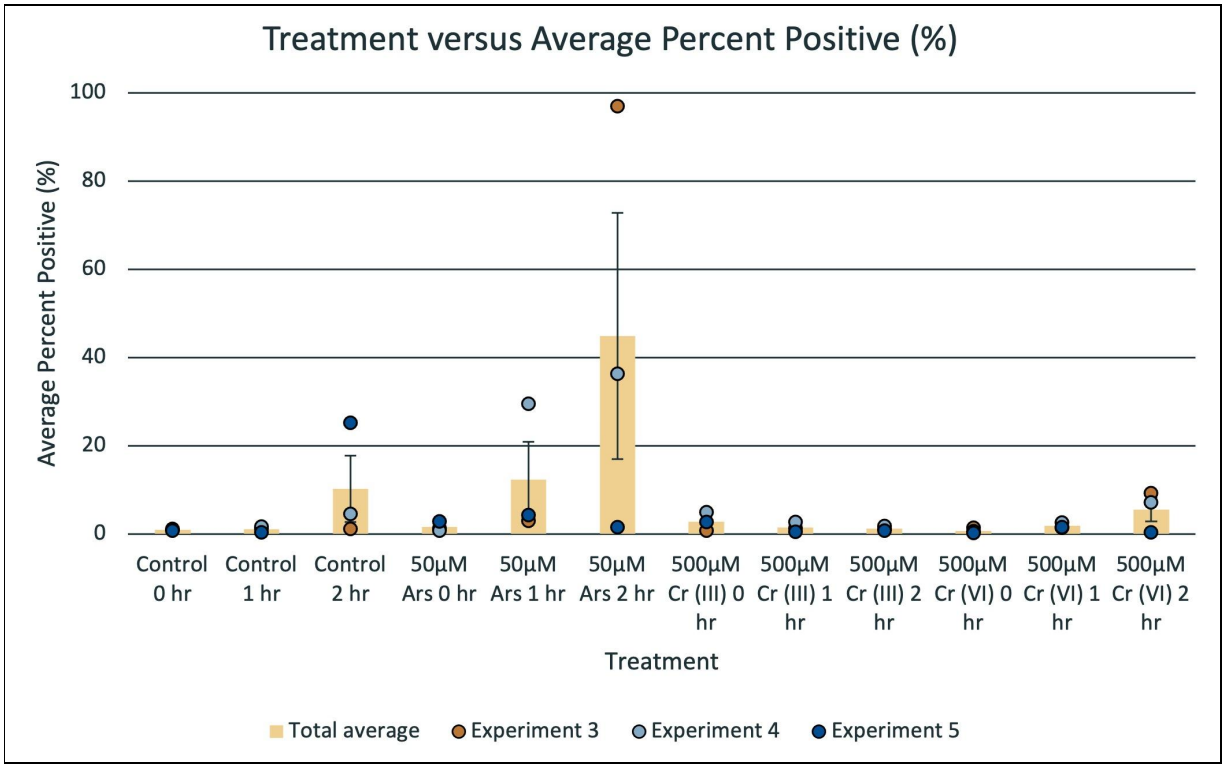

Figure 4: Stress granule formation in response to acute exposure of U2OS-DS cells to chromium III and VI. Cells were treated with 50 µM solutions for arsenic or 500 µM solutions of chromium III and VI for 0-2 hours and 3 replicates were performed. Error bars represent standard error and data points for each experiment are marked on the bars.

Investigating the Role of eIF2α Relation to Chromium Stress

The stress response is characterized by the phosphorylation of eukaryotic initiation factor-2α (eIF2α), which occurs on serine 51 in response to the activation of one of four eIF2α kinases (Humeau et al., 2020). Studies have shown that arsenite, our positive control, activates EIF2AK1, or commonly known as heme-regulated inhibitor (HRI). Mutant HAP1-S51A cells treated with arsenite are unable to phosphorylate serine 51 of eIF2α, inhibiting stress granule formation. Therefore, the wildtype cells would form stress granules and the mutant cells would not. Therefore, to investigate the specific pathway of stress-induced translational control induced by chromium, a drug exposure assay was conducted on both wild-type and mutant HAP1 cells.

Two replicates of an acute drug exposure assay, were conducted for wild-type and mutated S51A HAP1 cells. Similar to Figure 4, the concentrations of each treatment, arsenite, Cr III, and Cr VI, remained the same as well as the controls. In contrast, the treatments were incubated for 2 hours rather than one hour intervals. Figure 5 below illustrates that there is little to no stress granule

formation in HAP1-S51A cells. When treated with Cr VI, HAP1-S51A cells on average formed about 1% of stress granules. Similarly, both chromium variants caused about 1% or less stress granule formation on HAP1-WT cells. This percentage is not significant enough to provide evidence to either support or oppose the hypothesis. When treated with arsenite, HAP1-WT had a 55% average percent positive. As seen before, 50 µM of arsenite is around the stress granule formation threshold. Thus, it can form a wide range of results as indicated by the two data points and large error bar. In contrast, HAP1-S51A cells treated with arsenite failed to form any stress granules, which was expected for the positive control.

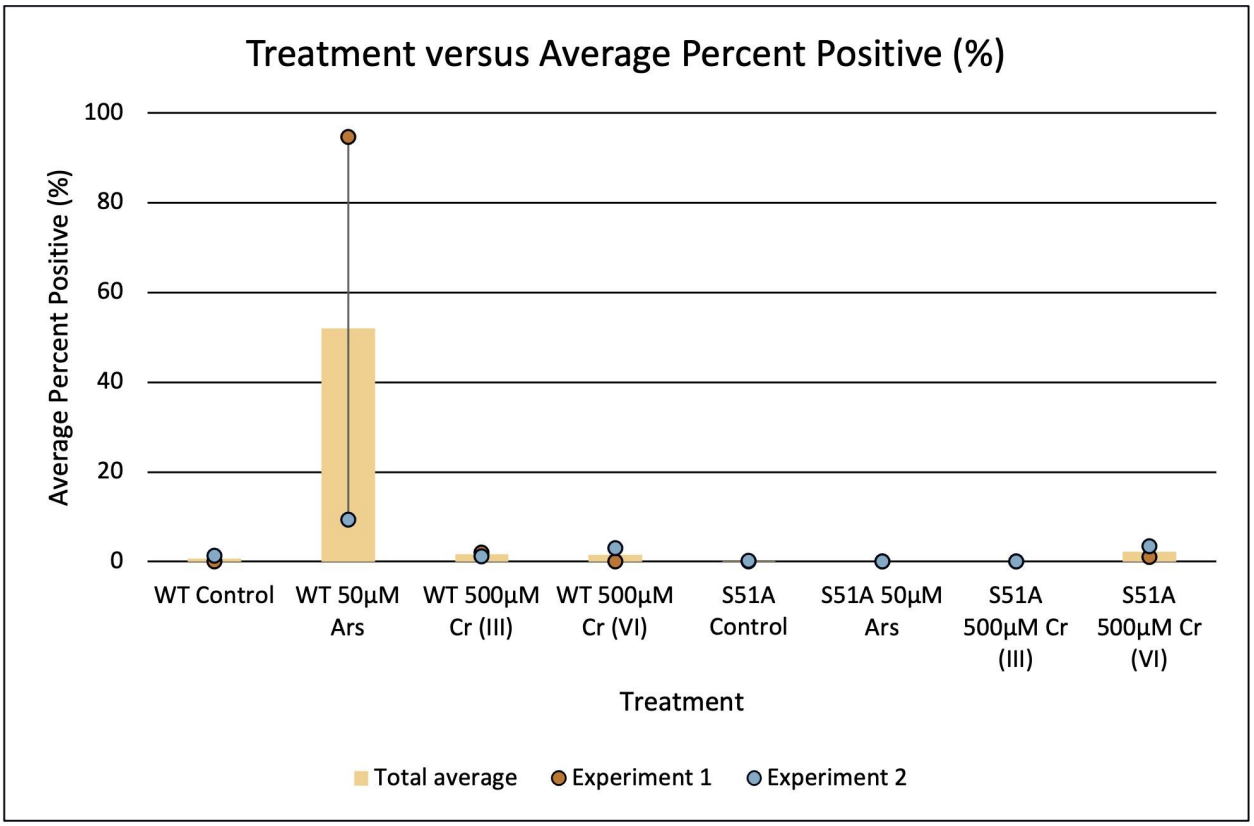

Figure 5: Stress granule formation in response to acute exposure of HAP1 wild-type and mutated S51A cells to chromium III and VI. Cells were treated with 50 µM solutions for arsenic or 500 µM solutions of chromium III and VI for 2 hours and 2 replicates were performed. Error bars represent standard error and data points for each experiment are marked on the bars.

Doubled Chromium Concentration Does Not Greatly Influence Stress Granule Formation

Since there was such low stress granule formation in response to chromium III and VI (Figure 5), Figure 6 illustrates the effects of twice as much chromium concentration (1 M) on wild-type and mutated S51A HAP1 cells. The trend of stress granule formation for HAP1-WT cells and no stress granules for S51A cells was not seen in this experiment. Both negative controls were

successful in no stress granule formation. In contrast to the trend mentioned, the positive control of arsenite indicated opposite results such that the wildtype cells were not effective in forming stress granules and about 18% of the S51A cells formed stress granules. When treated with Cr III, 2% of WT cells formed stress granules and its S51A counterpart lacked stress granules, following the trend. Both cell types treated with Cr VI resulted in 4.6% stress granule formation which does not follow the trend.

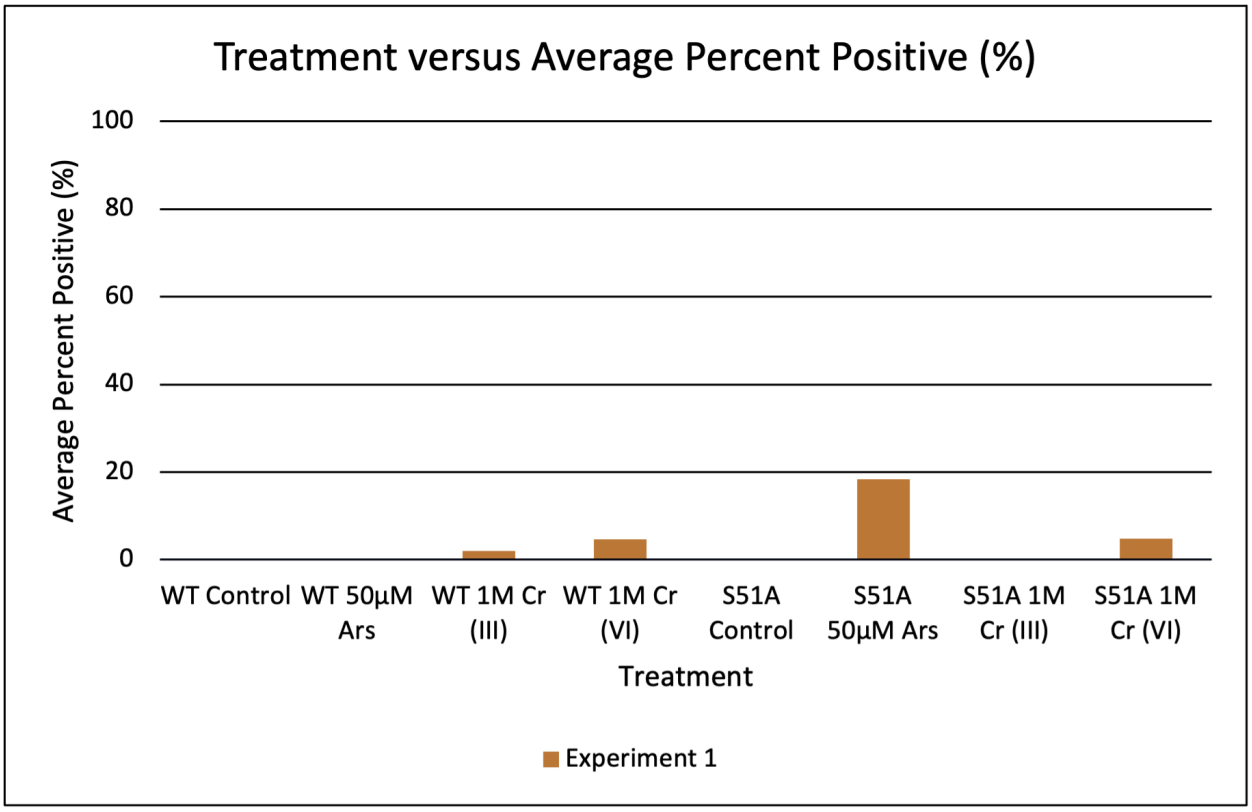

Figure 6: Stress granule formation in response to acute exposure of HAP1 wild-type and mutated S51A cells to chromium III and VI. Cells were treated with 50 µM solutions for arsenic or 1 M solutions of chromium III and VI for 2 hours and 1 replicate was performed.

Cr VI but not Cr III Causes Phosphorylation of eIF2α

Following an acute exposure assay on HAP1 WT and S51A cells (Figure 5), a Western blot was performed to qualitatively determine the phosphorylation state of eIF2α in response to the according treatment. When the Western blot was first stained for phosphorylated eIF2α (Figure 7; top), bands were present in lanes 2 (WT arsenite) and 4 (S51A Cr VI). These two lanes have bands of similar width and opacity, indicating a similar amount of protein (p-eIF2α) present in each sample. The remaining lanes lacked any bands indicating phosphorylation of eIF2α. Once the Western blot was stained with total eIF2α (Figure 7; bottom), each lane had a band present.

It can be observed from the bottom blot that all samples have eIF2α but only those treated with Ars or Cr VI (lanes 2 and 4) have more phosphorylated eIF2α than the untreated control (lane 1). In contrast, Cr III doesn't seem to cause phosphorylation (lane 3). In lanes 5-8 eIF2α cannot be phosphorylated, which proves the bands seen in the top blot are specific to eIF2α. Lane 9 contained sample spillover from lane 8, thus the band is fainter than others surrounding it.

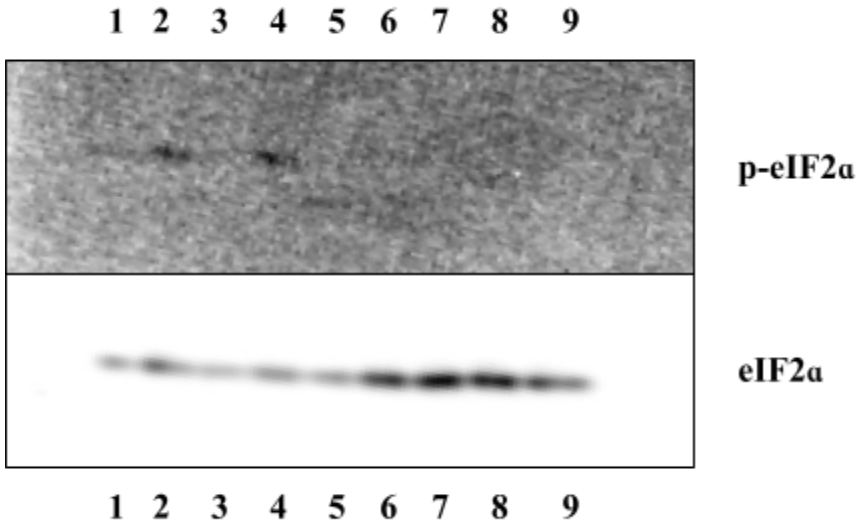

Figure 7: Western blot of acute exposure assay using HAP1 WT and S51A cells, stained for phosphorylated eIF2α (top) and total eIF2α (bottom). Wildtype (lanes 1-4) and S51A (lanes 5-9) cells treated with: negative control (lanes 1 and 5), arsenite (lanes 2 and 6), chromium III (lanes 3 and 7), and chromium VI (lanes 4, 8, and 9). One replicate was performed.

Discussion

U2OS-DS Acute Exposure Assay

As the hypothesis formed before the experiments predicted, Cr III and Cr VI were both responsible for stress granule formation and Cr VI had higher toxicity than Cr III in mammalian cells. However, Cr III did not seem to cause significant stress granule formation. Although Cr VI formed a higher percentage of SGs, it was still very modest at 2 hours of exposure. This result was better observed at U2OS-DS cells but was not well replicated in HAP-1 cells. Later, it was hypothesized that cells would form more stress granules as time passes. It was predicted that the longer a cell is under a stress condition, they may form a greater amount of stress granules. In order to observe a gradual increase in stress granule formation, the treatments were applied to the cells at 0, 1, or 2 hours in a similar fashion as the prior experiment. Data shown in Figure 4 helped conclude that this hypothesis was somewhat consistent with results from the hourly experiments. The Cr III treatment did not support the hypothesis since stress granule formation was incredibly low and no trend could be determined. The average percentages positive for all three time points were under 2%. This was not enough to conclude whether stress granule formation increased over time. The Cr VI treatment supported the hypothesis and showed a clear increase in stress granule formation over time, changing from roughly 1 to 5%. However, it was observed that an increase in stress granule amount was not relatively high compared to the positive control Arsenite at the same concentration. Overall, U2OS-DS cells produced stress granules when treated with Cr III and Cr VI and the number of stress granules increased as time passed for cells treated with Cr VI.

HAP1-WT and -S51A Acute Exposure Assay and Western Blot

As mentioned before, arsenite is known to use the eIF2α pathway and this can be supported by the use of HAP1-WT and -S51A cells. The wildtype is able to phosphorylate eIF2α, leading to stress granule formation, whereas the mutant cannot phosphorylate and thus cannot form stress granules. Thus, there should be a trend of stress granules for wildtype samples and none for mutant samples. The data indicated neither support or oppose the hypothesis that chromium variants use the eIF2α pathway of stress-induced translational control. Stress granule formation in response to chromium III and VI were low to begin with, 1.6% and 4.7% respectively (Figure 3). Although the trend was seen in Figure 5, the percentages were about 1% for each chromium variant and were not significant enough to support the hypothesis. Additionally, Figure 6 showed unanticipated results such that HAP1-S51A cells had stress granules when it was expected to be lacking. One replicate of the experiment was conducted, thus if given time for additional trials, these results could be improved and support or opposition for the hypothesis can be determined. While counting cells on coverslips for Figure 5 and 6 experiments, it was noted that some coverslips have more clumped cells than others where cells were hard to find. Perhaps the chromium variants kill the cells, which may explain the lack of stress granules formed. To

determine such, further assays that stain for live and dead cells can be performed to confirm or deny this theory.

Figure 7 indicated eIF2α phosphorylation in two wildtype samples, arsenite and Cr VI, and none in the control and the Cr III samples. As expected, no eIF2α phosphorylation was seen in any of the mutant samples. Typically phosphorylation levels indicated in Western blots are representative of stress granule formation for the samples. Interestingly, the Western blot conducted showed similar amounts of phosphorylation for arsenite and Cr VI in the two wildtype samples, yet the stress granule formation for Cr VI was much less than arsenite. Therefore, this figure loosely supports the hypothesis, but may not be enough to fully support it. Again, additional time and trials may be able to further support the hypothesis.

References

Abdulla, E. M., & Campbell, I. C. (1997). Studies of Neurotoxicity in Cellular Models. In Vitro Methods in Pharmaceutical Research,155-180. doi:10.1016/b978-012163390-5.50008-9

Anderson, P., & Kedersha, N. (2002, August 15). Stressful initiations *J Cell Sci* (2002) 115 (16): 3227–3234, https://doi.org/10.1242/jcs.115.16.3227

Anderson, P., & Kedersha, N. (2008). Stress granules: The tao of rna triage. *Trends in Biochemical Sciences, 33*(3), 141-150. doi:10.1016/j.tibs.2007.12.003

Arner, E. (2012, June 11). Redox cycling. Retrieved October 19, 2020, from http://genomics.unl.edu/RBC_2012/COURSE_FILES/mon5.pdf

Arora, M. (2013). Cell culture media: A review. *Materials and Methods, 3*. doi:10.13070/mm.en.3.175

Bagchi, D., Bagchi, M., & Stohs, S. J. (2001). Chromium (VI)‐induced oxidative stress, apoptotic cell death and modulation of p53 tumor suppressor gene. Molecular and Cellular Biochemistry,222(1/2), 149-158. doi:10.1023/a:1017958028256

Collier, N. C., & Schlesinger, M. J. (1986). The dynamic state of heat shock proteins in chicken embryo fibroblasts. *Journal of Cell Biology, 103*(4), 1495-1507. doi:10.1083/jcb.103.4.1495

Epa.gov. (2000, January 22). Chromium Compounds. Retrieved October 19, 2020, from https://www.epa.gov/sites/production/files/2016-09/documents/chromium-compounds.pdf

Ercal, N. S., Gurer-Orhan, H. S., & Aykin-Burns, N. S. (2001). Toxic Metals and Oxidative Stress Part I: Mechanisms Involved in Me-tal induced Oxidative Damage. Current Topics in Medicinal Chemistry,1(6), 529-539. doi:10.2174/1568026013394831

Feng, X., & Koh, D. W. (2013). Roles of poly(adp-ribose) glycohydrolase in dna damage and apoptosis. *International Review of Cell and Molecular Biology,* 227-281. doi:10.1016/b978-0-12-407696-9.00005-1

Fulda, S., Gorman, A. M., Hori, O., & Samali, A. (2010). Cellular Stress Responses: Cell Survival and Cell Death. *International Journal of Cell Biology*, 2010, 1-23. doi:10.1155/2010/214074

Gibb, H. J., Lees, P. S., Pinsky, P. F., & Rooney, B. C. (2000). Lung cancer among workers in chromium chemical production. *American Journal of Industrial Medicine, 38*(2), 26-115. doi:10.1002/1097-0274(200008)38:23.0.co;2-y

Humeau, J., Leduc, M., Cerrato, G., Loos, F., Kepp, O., & Kroemer, G. (2020). Phosphorylation of eukaryotic initiation factor-2α (eif2α) in autophagy. Cell Death & Disease, 11(6). doi:10.1038/s41419-020-2642-6

Kedersha, N., Ivanov, P., & Anderson, P. (2013). Stress granules and cell signaling: More than just a passing phase? *Trends in Biochemical Sciences, 38*(10), 494-506. doi:10.1016/j.tibs.2013.07.004

Lazarova, N., Krumova, E., Stefanova, T., Georgieva, N., & Angelova, M. (2014). The oxidative stress response of the filamentous yeastTrichosporon cutaneumR57 to copper, cadmium and chromium exposure. *Biotechnology & Biotechnological Equipment*, 28(5), 855-862. doi:10.1080/13102818.2014.965020

National Institutes of Health. (2020, October 1). Office of Dietary Supplements - Chromium. Retrieved December 05, 2020, from https://ods.od.nih.gov/factsheets/Chromium-HealthProfessional/

Nostramo, R., & Herman, P. K. (2016). Deubiquitination and the regulation of stress granule assembly. *Current genetics, 62*(3), 503–506. https://doi.org/10.1007/s00294-016-0571-9

OSHA.gov. (n.d.). Department of Labor logo UNITED STATESDEPARTMENT OF LABOR. Retrieved October 19, 2020, from https://www.osha.gov/hexavalent-chromium

Poljšak, B., & Milisav, I. (2012). Clinical implications of cellular stress responses. *Bosnian Journal of Basic Medical Sciences*, 12(2), 122. doi:10.17305/bjbms.2012.2510

Appendix

Appendix A: Raw data from chromium III, chromium VI, and arsenite acute exposure comparison assay

1 drug treatment completed 9/27/2020

		Vivian's counts		Furkan's counts				
Slide #	Treatment	Yes	No	Yes	No	V percent positive (%)	F percent positive (%)	Average percent positive (%)
1	500µM Ars	260	0	335	2	100.000	99.407	99.70326409
2	500µM Cr (III)	0	279	3	328	0.000	0.906	0.4531722054
3	500µM Cr (VI)	3	288	32	250	1	11	6.189222783
4	control	1	270	3	272	0.369	1.091	0.7299563905
5	500µM Ars	252	0	332	8	100.000	97.647	98.82352941
6	500µM Cr (III)	1	289	12	275	0.345	4.181	2.263006128
7	control	3	293	6	289	1.014	2	1.523705909
8	500µM Cr (VI)	2	306	25	268	0.649	8.532	4.590886929

Treatment	Avg. % pos.
Control	1.12683115
500µM Ars	99.26339675
500µM Cr (III)	1.358089167
500µM Cr (VI)	5.390054856

2 drug treatments completed 10/3/2020

Original blue tape

		Vivian's counts		Furkan's counts				
Slide #	Treatment	Yes	No	Yes	No	V percent positive (%)	F percent positive (%)	Average percent positive (%)
1	Control	4	268	7	300	1.471	2.280	1.875359264
2	Control	11	253	30	300	4.167	9.091	6.628787879
3	500µM Ars	295	2	300	3	99	99	99.16825016
4	500µM Cr (VI)	5	280	5	300	1.754	1.639	1.696865114
5	500µM Cr (III)	3	278	3	300	1.068	0.990	1.028857334
6	500µM Ars	301	2	300	2	99.340	99.338	99.33884117
7	500µM Cr (III)	2	310	10	300	0.641	3	1.933416046
8	500µM Cr (VI)	1	255	48	300	0.391	13.793	7.091864224

Treatment	Avg. % pos.
Control	4.252073572
500µM Ars	99.25354566
500µM Cr (III)	1.48113669
500µM Cr (VI)	4.394364669

Original pink tape

		Vivian's counts		Furkan's counts				
Slide #	Treatment	Yes	No	Yes	No	V percent positive (%)	F percent positive (%)	Average percent positive (%)
1	control	4	290	10	300	1.361	3.226	2.293175335
2	500µM Cr (III)	0	290	10	300	0.000	3.226	1.612903226
3	500µM Cr (VI)	14	252	2	300	5	1	2.962704775
4	500µM Ars	263	0	300	1	100.000	99.668	99.83388704
5	control	12	277	5	300	4.152	1.639	2.895796699
6	500µM Cr (VI)	7	259	30	300	2.632	9.091	5.861244019
7	500µM Ars	304	1	300	2	99.672	99	99.50493975
8	500µM Cr (III)	13	263	2	300	4.710	0.662	2.686198292

Treatment	Avg. % pos.
Control	2.594486017
500µM Ars	99.66941339
500µM Cr (III)	2.149550759
500µM Cr (VI)	4.411974397

Appendix B: Raw data from hourly acute exposure comparison assay

1 drug treatment completed 10/17/2020

EXPERIMENT 3

		Vivian's counts		Furkan's counts				
Slide #	Treatment	Yes	No	Yes	No	V percent positive (%)	F percent positive (%)	Average percent positive (%)
1	Control, 2hr	1	220	6	342	0.452	1.724	1.088313309
2	Control, 0hr	0	262	5	296	0.000	1.661	0.8305647841
3	50 Ars, 0hr	2	235	5	313	1	2	1.20810445
4	50 Ars, 2hr	198	3	278	13	98.507	95.533	97.02005437
5	500 Cr VI, 0hr	1	218	8	346	0.457	2.260	1.358254005
6	500 Cr VI, 2hr	18	196	30	268	8.411	10.067	9.239164524
7	50 Ars, 1hr	6	217	10	301	2.691	3	2.953008522
8	Control, 1hr	3	266	3	286	1.115	1.038	1.07665196
9	500 Cr III, 0hr	0	263	5	302	0.000	1.629	0.8143322476
10	500 Cr VI, 1hr	2	279	6	274	0.712	2.143	1.427300458
11	500 Cr III, 1hr	3	292	5	320	1.017	1.538	1.277705346
12	500 Cr III, 2hr	3	212	2	262	1.395	0.758	1.076462297

1 drug treatment completed 10/24/2020

EXPERIMENT 4

		Vivian's counts		Furkan's counts				
Slide #	Treatment	Yes	No	Yes	No	V percent positive (%)	F percent positive (%)	Average percent positive (%)
1	500 Cr III, 1 hr	7	193	5	262	3.500	1.873	2.686329588
2	500 Cr VI, 2 hr	21	189	11	245	10.000	4.297	7.1484375
3	500 Cr III, 0 hr	14	195	8	245	7	3	4.930309965
4	50 Ars, 1 hr	77	134	52	178	36.493	22.609	29.55079332
5	500 Cr VI, 1 hr	8	212	4	273	3.636	1.444	2.540203479
6	50 Ars, 2 hr	96	125	73	178	43.439	29.084	36.26128968
7	Control, 2 hr	13	201	7	225	6.075	3	4.546003867
8	500 Cr III, 2 hr	6	216	2	246	2.703	0.806	1.754577158
9	Control, 1 hr	6	230	2	289	2.542	0.687	1.614829052
10	Control, 0 hr	4	240	2	290	1.639	0.685	1.162137885
11	50 Ars, 0 hr	1	236	3	301	0.422	0.987	0.7043915168
12	500 Cr VI, 0 hr	2	205	1	283	0.966	0.352	0.6591481255

1 drug treatment completed 11/3/2020

EXPERIMENT 5

		Vivian's counts		Furkan's counts				
Slide #	Treatment	Yes	No	Yes	No	V percent positive (%)	F percent positive (%)	Average percent positive (%)
1	500 Cr VI, 2 hr	0	233	2	286	0.000	0.694	0.3472222222
2	500 Cr VI, 1 hr	3	198	3	201	1.493	1.471	1.481562774
3	50 Ars, 1 hr	8	198	12	243	4	5	4.294688749
4	50 Ars, 2 hr	4	208	2	185	1.887	1.070	1.478155585
5	Control, 2 hr	69	163	48	185	29.741	20.601	25.17111884
6	50 Ars, 0 hr	4	218	8	192	1.802	4.000	2.900900901
7	Control, 1 hr	0	225	2	237	0.000	1	0.4184100418
8	Control, 0 hr	1	225	2	202	0.442	0.980	0.7114350165
9	500 Cr III, 0 hr	4	228	8	206	1.724	3.738	2.731227844
10	500 Cr III, 1 hr	2	277	1	257	0.717	0.388	0.5522213887
11	500 Cr III, 2 hr	1	207	2	176	0.481	1.124	0.8021823682
12	500 Cr VI, 0 hr	1	251	0	210	0.397	0.000	0.1984126984

Appendix C: Raw data from wild-type versus. S51A mutant HAP1 cells acute exposure comparison assay

1 drug treatment completed 2/17/2021								
EXPERIMENT 1								
		Vivian's counts		Furkan's counts				
Slide #	Treatment	Yes	No	Yes	No	V percent positive (%)	F percent positive (%)	Average percent positive (%)
1A	S51A Cr VI	4	301	2	275	1.311	0.722	1.016748535
1B	WT Cr VI	0	266	0	304	0.000	0.000	0
2A	WT control	0	280	0	299	0	0	0
2B	S51A control	0	295	0	263	0.000	0.000	0
3A	WT Cr III	3	259	8	270	1.145	2.878	2.011368005
3B	S51A Cr III	0	317	0	293	0.000	0.000	0
4A	S51A Ars	0	295	0	309	0.000	0	0
4B	WT Ars	259	18	278	12	93.502	95.862	94.68193701
1 drug treatment completed 3/3/2021								
EXPERIMENT 2								
		Vivian's counts		Furkan's counts				
Slide #	Treatment	Yes	No	Yes	No	V percent positive (%)	F percent positive (%)	Average percent positive (%)
1	WT Cr III	2	307	5	274	0.647	1.792	1.219681943
2	S51A Cr III	0	275	0	283	0.000	0.000	0
3	WT Control	5	294	3	290	2	1	1.348065794
4	S51A Control	1	346	0	327	0.288	0.000	0.144092219
5	WT Ars	25	290	32	264	7.937	10.811	9.373659374
6	S51A Ars	0	326	0	299	0.000	0.000	0
7	WT Cr VI	13	368	8	285	3.412	3	3.071224459
8	S51A Cr VI	11	250	9	312	4.215	2.804	3.509148852

Appendix D: Raw data from HAP1 cells and double chromium concentration acute exposure comparison assay

1 drug treatment completed 3/10/2021								
EXPERIMENT 1								
		Vivian's counts		Furkan's counts				
Slide #	Treatment	Yes	No	Yes	No	V percent positive (%)	F percent positive (%)	Average percent positive (%)
1	S51A Cr III	1	265	0	302	0.376	0.000	0.1879699248
2	WT C	0	328	0	310	0.000	0.000	0
3	S51A Cr VI	5	339	8	296	1	3	2.04253366
4	WT Cr III	13	274	15	300	4.530	4.762	4.645760743
5	S51A Ars	1	344	0	321	0.290	0.000	0.1449275362
6	WT Ars	64	266	51	243	19.394	17.347	18.37043908
7	S51A C	0	297	0	314	0.000	0	0
8	WT Cr VI	14	243	12	287	5.447	4.013	4.730424372